Electronic Supplementary Material (ESI) for Physical Chemistry Chemical Physics.

Electronic Supplementary Information:

On photocatalytic cycle of water splitting with small manganese oxides
and the roles of water cluster as a direct resource of oxygen molecules

Kentaro Yamamoto* and Kazuo Takatsuka†
Fukui Institute for Fundamental Chemistry, Kyoto University,
Takano-Nishihiraki-cho 34-4, Sakyou-ku, Kyoto 606-8103, Japan

December 8, 2017

Contents

---

*email: `kyamamoto@fukui.kyoto-u.ac.jp`
†email: `kaztak@fukui.kyoto-u.ac.jp`, corresponding author

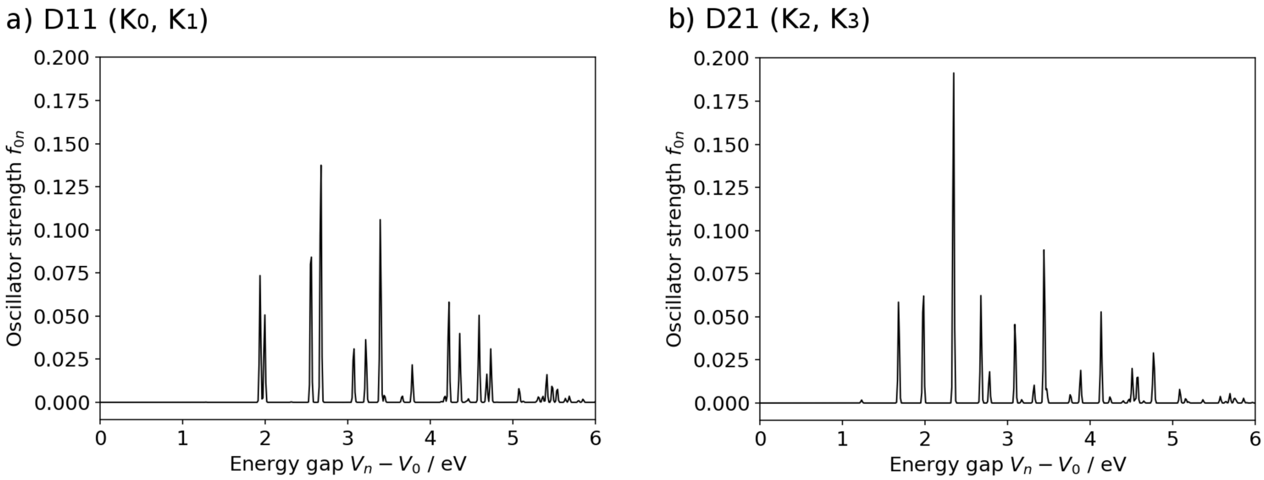

Figure S1: Oscillator strength f_{0n} between the ground and excited states as a function of energy gap $V_n - V_0$ for (a) D11 and (b) D21.

S1 CPEWT in triplet states involving a hydrogen-bond network

S1.1 Oscillator strength

In our dynamical analysis, the initial electron-wavepackets are supposed to be photoexcited states. The oscillator strength f_{0n} of D11 and D21 (see Fig. 8 in the main text) as a function of energy gap $V_n - V_0$ is shown in Fig. S1. We observe photo-excitable states around 2 – 3 eV in energy gap. The initial electron-wavepacket is prepared by coherently superposing these photo-excited states weighted with the oscillator strength, and the mean potential energy is approximately equal to 3 eV.

S1.2 Connecting the electron-wavepackets with different reference MOs

As mentioned in the main text, the electron wavepacket dynamics undergoes discontinuity of the reference MOs to technically break down the proper time-evolution. We can conveniently connect the electron-wavepackets expressed by the different sets of reference MOs by maximizing the overlap of them instead of employing multi-reference methods. See Fig. S2 for each two sets of MOs for D11 and D21. In the present work, the electron-wavepacket $|\Psi_{\text{elec}}\rangle$ is expanded in the series of reordered adiabatic states $|\Phi_\alpha\rangle$:

$$|\Psi_{\text{elec}}\rangle = \sum_{\alpha} C_\alpha |\Phi_\alpha\rangle \tag{1}$$

Here "reordered" means that the order of the adiabatic states that is originally ascending order in energy is changed so that the overlap of $|\Psi_{\text{elec}}\rangle$ with that of the previous point along the time-evolution becomes as close to the unit matrix up to the phase as possible. Recall that $\{C_\alpha\}$ is the time-dependent coefficients. The phase of each state is also reversed if necessary for continuity. We can conveniently

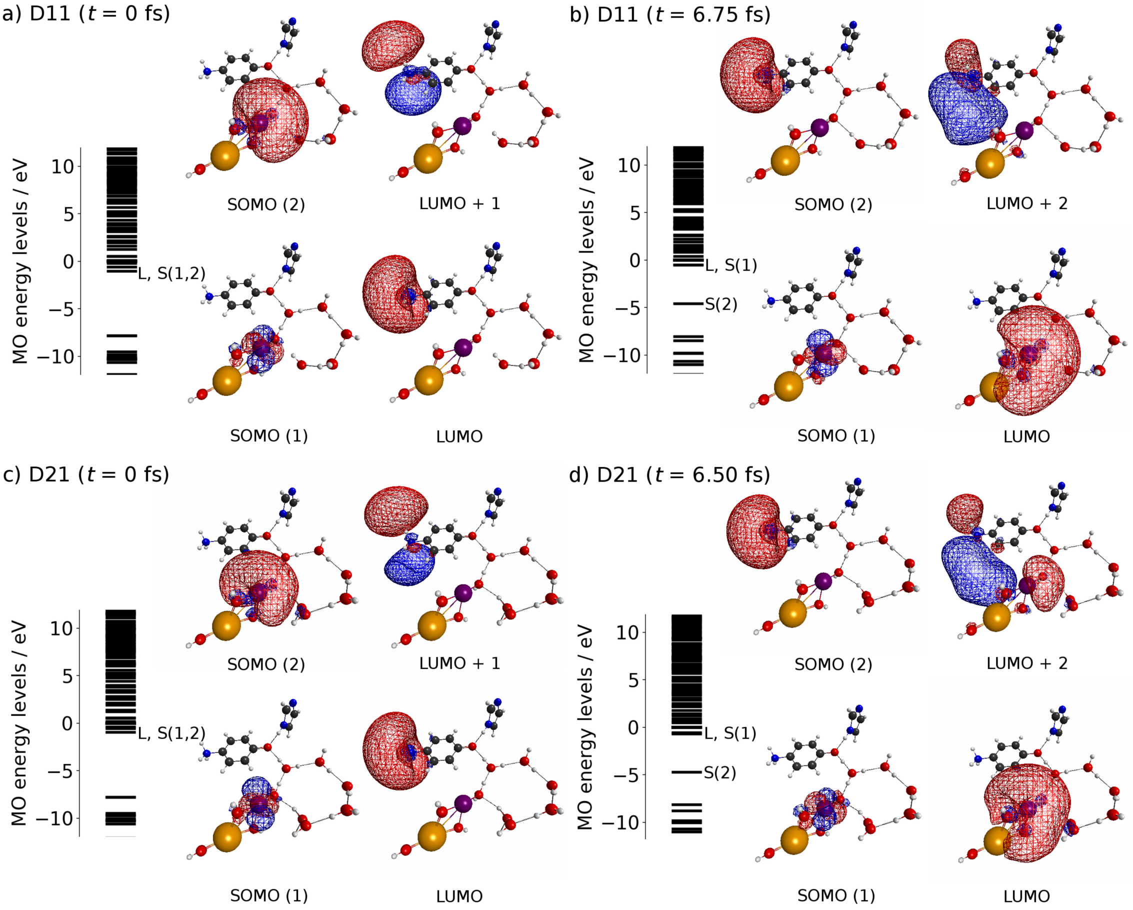

Figure S2: Spatial distribution of the frontier MOs at selected times. (a) System D11 at $t = 0$ fs, in which two SOMOs and two LUMOs are quasi-degenerate. (b) System D11 at $t = 6.5$ fs. At this point the MO characters switch from (a) to (b). SOMO(1) and LUMO are interchanged. It affects the rest of the MOs to break the one-to-one correspondence among them along the time evolution. (c) and (d) are those for D21.

avoid the divergence in derivatives at a conical intersection by means of this reordering procedure. Note that the reordered adiabatic states are still the eigenstates of the electronic Hamiltonian $\hat{H}^{(\mathrm{el})}$. The set of reference MOs switches from that involving the Mn d-shell as one of the SOMOs to that bearing the Rydberg-like state.

In practice, the continuity of electron-wavepacket is materialized by means of following method. Let us define the overlap of the electron-wavepacket represented in the different sets of reference MOs:

$$\langle \Psi^1_{\mathrm{elec}} | \Psi^2_{\mathrm{elec}} \rangle = \sum_{\alpha\beta} C^{1*}_{\alpha} C^2_{\beta} \langle \Phi^1_{\alpha} | \Phi^2_{\beta} \rangle \tag{2}$$

in which the superscripts 1 and 2 specify the set of reference MOs. The problem we need to solve is to optimize $\{C^2_{\beta}\}$ for given $\{C^1_{\alpha}\}$ and $\{\langle \Phi^1_{\alpha} | \Phi^2_{\beta} \rangle\}$. We actually minimized the following function f

$$f(\{C^2_{\beta}\}) = -\mathrm{Re}(\langle \Psi^1_{\mathrm{elec}} | \Psi^2_{\mathrm{elec}} \rangle)^2 + \mathrm{Im}(\langle \Psi^1_{\mathrm{elec}} | \Psi^2_{\mathrm{elec}} \rangle)^2 + \lambda (1 - \sum_{\beta} |C_{\beta}|^2)^2 \tag{3}$$

with λ denotes the Lagrange undetermined multiplier relevant to the normalization. This function $f(\{C^2_{\beta}\})$ is solved numerically to obtain $\{C^2_{\beta}\}$ with which we restart the electron-wavepacket dynamics.

Technically it is not easy to evaluate the overlap matrix of the reordered adiabatic states $\langle \Phi^1_{\alpha} | \Phi^2_{\beta} \rangle$ for those given at mutually different nuclear positions. The reordered adiabatic states are further expanded in the series of configuration state functions (CSFs):

$$|\Phi_{\alpha}\rangle = \sum_{I}^{\mathrm{CSF}} C_{I\alpha} |\Phi_I\rangle \tag{4}$$

Thus the overlap matrix defined in Eq. (2) can be rewritten:

$$\begin{aligned} \langle \Psi^1_{\mathrm{elec}} | \Psi^2_{\mathrm{elec}} \rangle &= \sum_{\alpha\beta} C^{1*}_{\alpha} C^2_{\beta} \sum_{IJ}^{\mathrm{CSF}} C^{1*}_{I\alpha} C^2_{J\alpha} \langle \Phi^1_I | \Phi^2_J \rangle \\ &\approx \sum_{\alpha\beta} C^{1*}_{\alpha} C^2_{\beta} \sum_{IJ}^{\mathrm{CSF}} C^{1*}_{I\alpha} C^2_{J\alpha} \frac{1}{N_e} \sum_{ij}^{\mathrm{MO}} a^{IJ}_{ij} \langle \phi^1_i | \phi^2_j \rangle \end{aligned} \tag{5}$$

with ϕ^1_i for instance being a molecular orbital at the reference point 1. We have approximated the CSF overlap matrix in the second line. Here a^{IJ}_{ij} denotes the spin-free one-electron coupling constant and N_e does the number of electrons. [1] If the reference sets of MOs are the same as each other, this equation holds exactly. Although the approximated method of wavepacket connection is employed, properties such as charge and unpaired electron population can be smoothly connected (see Sec. S1.3). It indicates that this approximation sufficiently works in the present system.

S1.3 Time-evolution of the properties along the SET paths

As shown in Fig. S3a, conical intersections can be found in the excited states with the energy gap $V_n - V_0$ being around 3 eV. The conical intersection seen around $t = 4$ to 5 fs are especially important,

a) $V_n - V_0$, $|C_n|^2$

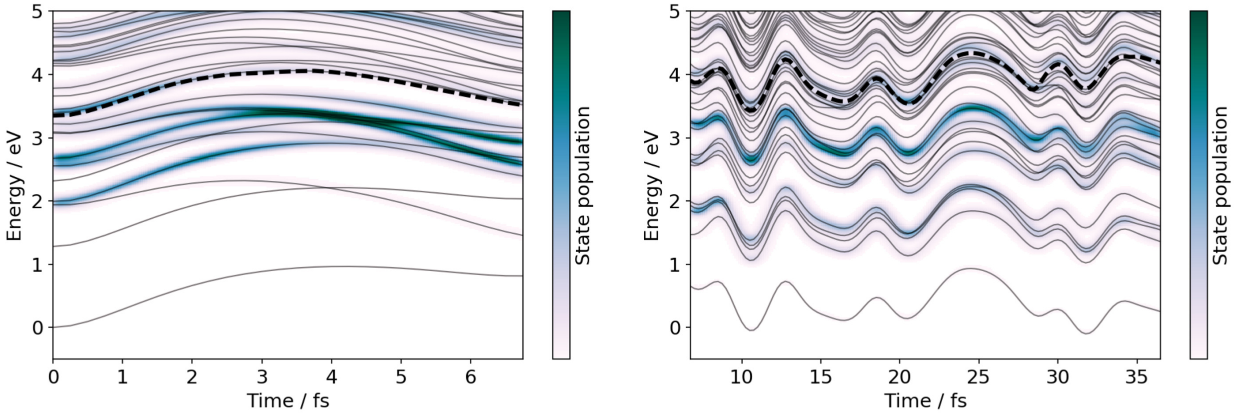

b) $R_{HA} - R_{HD}$

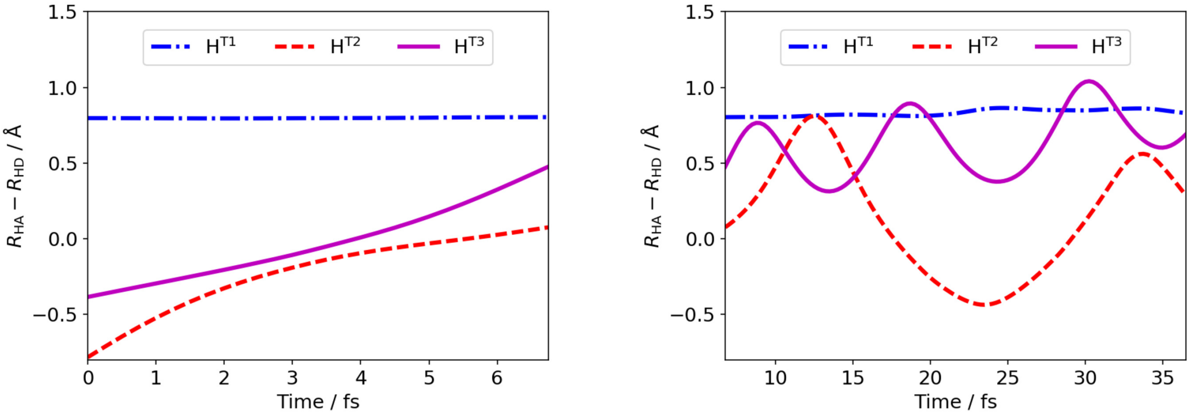

Figure S3: Time evolution of the selected properties along the SET path of D11 (K_0/K_1). The graphs belonging to the left and right columns use the reference sets of MOs of Fig. S2a and Fig. S2b, respectively. (a) Potential energy gap $V_n - V_0$ (solid lines), state population $|C_n|^2$ (pseudo color map), and SET mean potential $\langle V \rangle$ (dashed line). (b) $R_{\mathrm{HA}} - R_{\mathrm{HD}}$ to indicate H^n transfer.

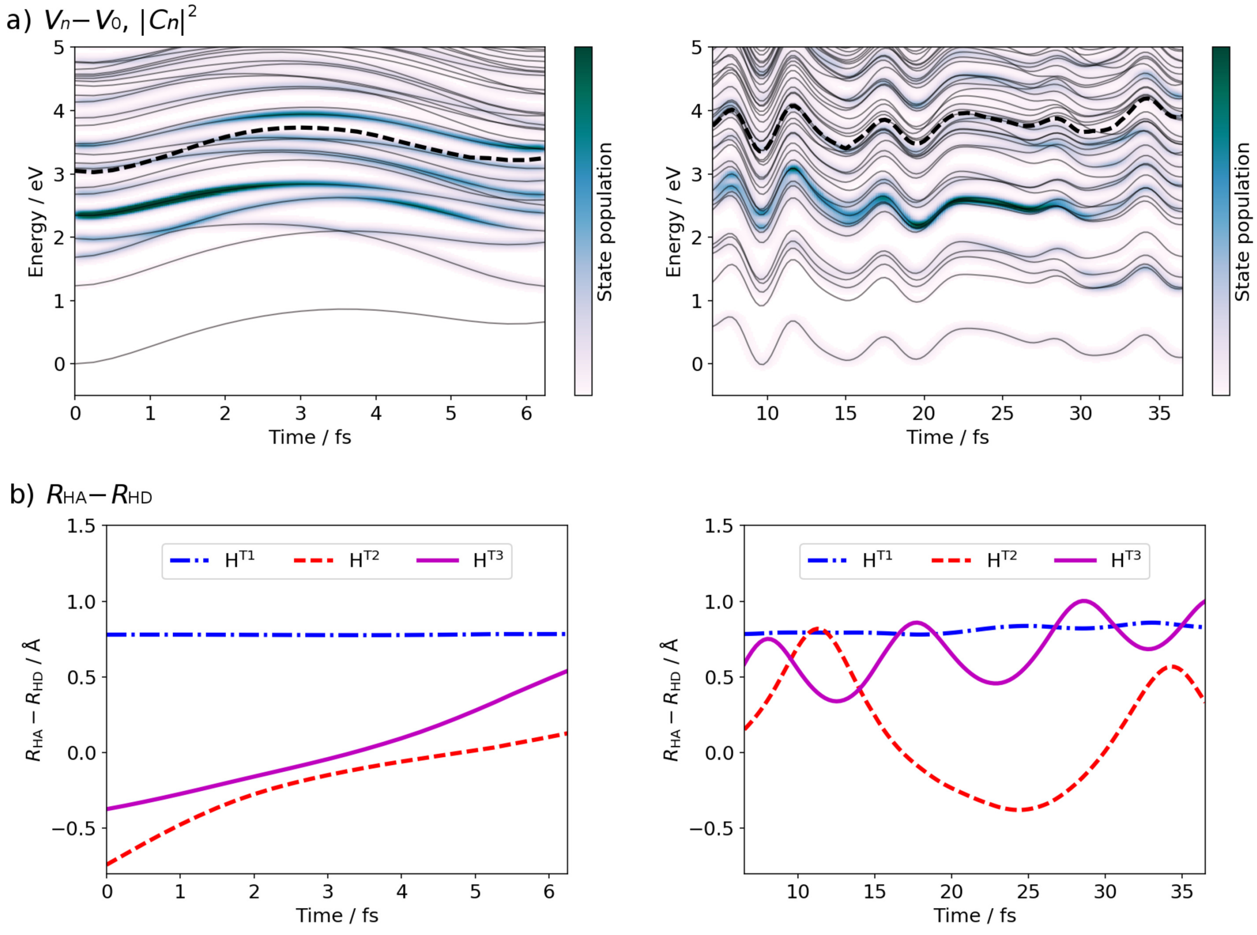

Figure S4: Time evolution of the selected properties along the SET path of D21 (K_2/K_3). The graphs belonging to the left and right columns use the MOs of Fig. S2c and Fig. S2d, respectively. (a) Potential energy gap $V_n - V_0$ (solid lines), state population $|C_n|^2$ (pseudo color map), and SET mean potential $\langle V \rangle$ (dashed line). (b) $R_{\mathrm{HA}} - R_{\mathrm{HD}}$ to indicate H^n transfer.

because they are one of the typical points relevant to the CPEWT. As shown in Fig. S3b, $R_{\mathrm{HA}} - R_{\mathrm{HD}}$ relevant to H^n $(n = 2, 3)$ transfer is around zero in both cases, in which R_{HA} and R_{HD} are internuclear distances between the proton–(acceptor atom) and proton–(donor atom) in the initial nuclear configuration, respectively. Passing across the point of $R_{\mathrm{HA}} - R_{\mathrm{HD}} = 0$ designates the proton transfer. H^3 is obviously accelerated toward the acceptor side almost at the same time as the nonadiabatic transition at $t = 4.3$ fs. It indicates that the proton transfer dynamically couples with the electron-wavepacket transfer. We find qualitatively the same results for D21 as shown in Fig. S4.

The electronic states of H^n $(n = 1, 2, 3)$ in the CPEWT can be characterized in a little more quantitatively by means of the "regional population analysis", in which the atomic populations in each region predefined within the super-molecule are individually summed up. [2–4] We first assign the total electron density and the unpaired electron density to the atoms by means of Löwdin's method

a) Q_M

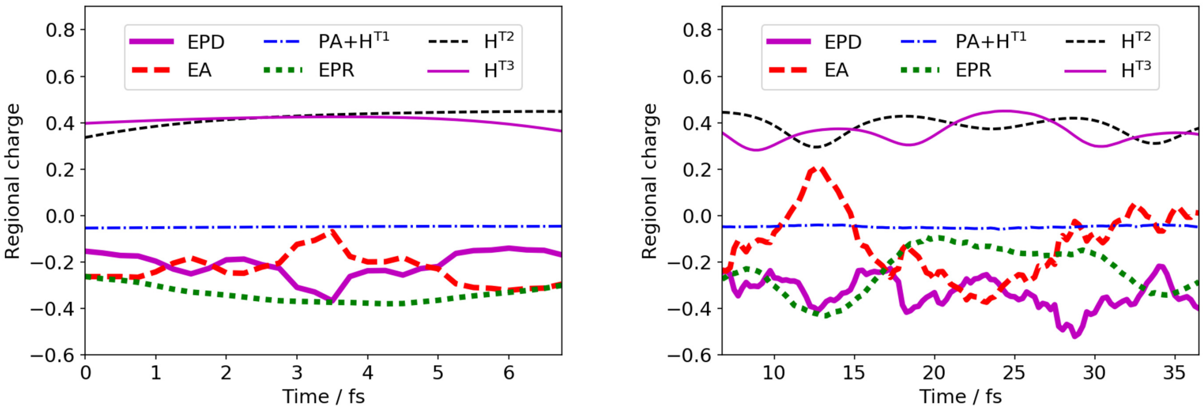

b) D_M

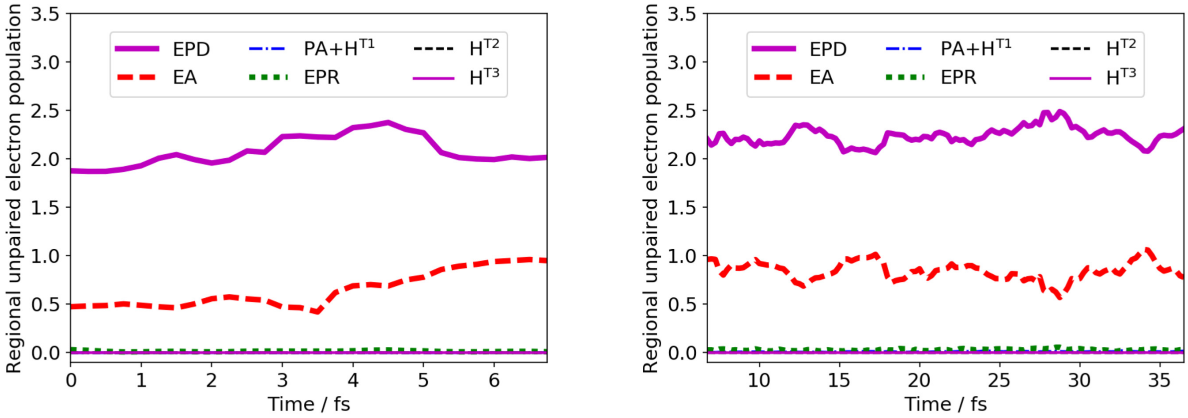

Figure S5: Time evolution of the selected properties along the SET path of D11 (K_0/K_1). The graphs belonging to the left and right columns use the reference sets of MOs of Fig. S2a and Fig. S2b, respectively. (a) Regional charge Q_M. (b) Regional unpaired electron population D_M.

to obtain atomic population. [5] Mulliken's original method [6] is known to be inappropriate for such a system that a basis set includes diffuse functions. The resulting regional populations are referred to as regional total electron population P_M and regional unpaired electron population D_M, with M denoting a region of the system. We actually utilize the regional charge $Q_M = Z_M - P_M$ instead of P_M for the sake of convenience, in which Z_M is the sum of nuclear charges in each region. The "regions" to distinguish the submolecular parts of the entire system are defined to be H^n ($n = 1, 2, 3$), the EPD, the EA, the PA, and the EPR (refer to Fig. 2 of the main text for the definitions). Q_M and D_M of D11 are shown in Fig. S5a and Fig. S5b, respectively. Q_M on H^n ($n = 1, 2, 3$) is all kept approximately +0.4, and D_M on them is kept virtually zero. This is the same situation as the previous study with the Y-shaped acceptor, and we can say that the relevant protons to the proton-relay transfer of the CPEWT locally move as if they are in the ground state. [4]

It is important to distinguish the CPEWT from the H radical transfer (H atom migration), because

a) Q_M

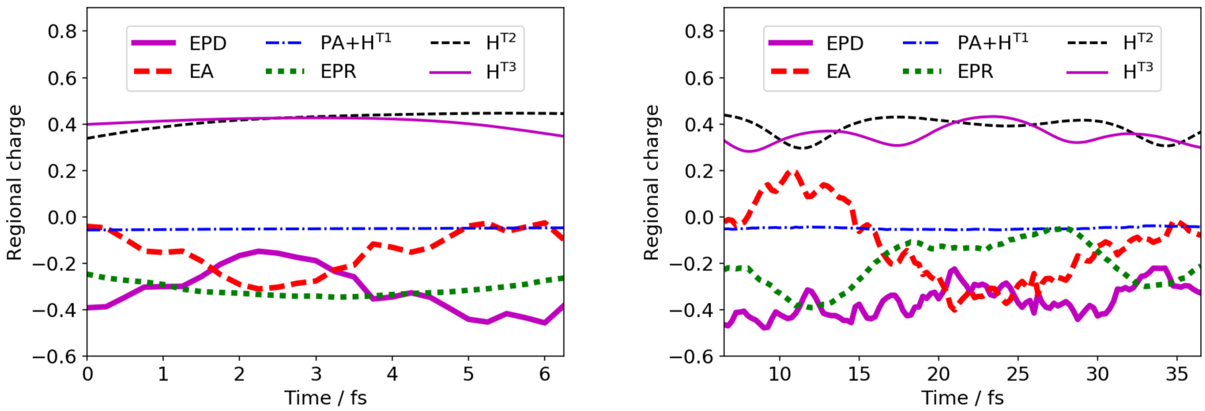

b) D_M

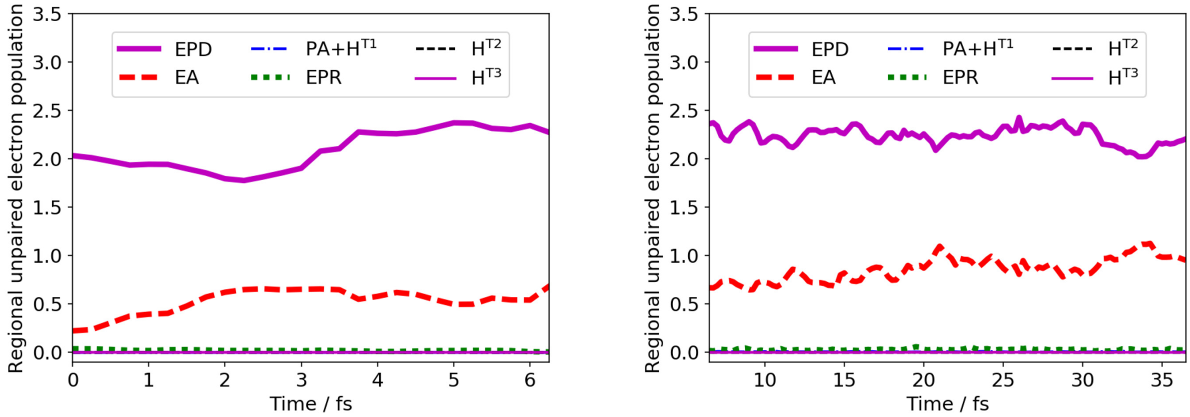

Figure S6: Time evolution of the selected properties along the SET path of D21 (K_2/K_3). The graphs belonging to the left and right columns use the reference sets of MOs of Fig. S2c and Fig. S2d, respectively. (a) Regional charge Q_M. (b) Regional unpaired electron population D_M.

only the former can induce charge separation by itself. One can make that distinction by closely looking at Q_M and D_M. If hydrogen atom migration actually takes place in the present H^n relay-transfer, Q_M and D_M on H^n should be virtually zero and unity, respectively. This is not the case in the present dynamics. We can find qualitatively the same results for D21 as shown in Fig. S6.

Table S1: Energies of each component for estimating the energy profile.

First group		Second group		
Component	Energy / eV	Component	Molecule[a)]	Energy / eV
^{3}[D11]	-55710.59	H_2O	^1H_2O	-2067.64
^{2}[D12]$^+$	-55708.42	EBf–e$^-$	$^1R^-$	-9357.17
^{2}[D13]$^+$	-55708.35	EBf	^2R	-9356.74
^{2}[D14]	-55695.96	PBf–H$^+$	^1RH	-9372.95
^{3}[D15]	-55678.91	PBf	$^1R^-$	-9357.17
^{3}[D21]	-57743.80	XEA	^2R	-9356.74
^{2}[D22]$^+$	-57741.72	XEA–e$^-$	$^1R^-$	-9357.17
^{2}[D23]$^+$	-57741.41	XPA	$^1R^-$	-9357.17
^{2}[D24]	-57729.22	XPA–H$^+$	^1RH	-9372.95
^{3}[D25]	-57712.86	O_2	$^3O_2$	-4068.82
^{1}[D11]	-55709.07			

a) R = CH_3–C_6H_4–O (4-methylphenyl)

S2 Energy profile for the series of reactions

S2.1 Energies of the first and the second groups

The total energy of each intermediate is estimated by summing up the energy of the first and the second groups (see Sec. 3.4.1 in the main text). Recall that the first group is defined to contain the EA, the PA, the EPD, the EPR, and H^n, and the second one consists of all the other parts including the XEA, the XPA, the EBf, and the PBf. The energies of the components of the first and the second groups are shown in Table S1. As for the first group, we optimize the geometries of the super molecules shown in Fig. 8 in the main text with the charge and the spin state indicated in Table S1. The spin multiplicity is basically chosen to be triplet if the number of electrons is an even number, and to be doublet if it is an odd number. One exception is ^{1}[D11], which is used to combine a triplet O_2 molecule to estimate energy profile, because a singlet EPD is left after the O=O bond formation. As for the second group, we use the geometry-optimized energy of the molecules listed in the column "Molecule" of Table S1. For the second group, the spin multiplicity is basically chosen to be singlet if the number of electrons is an even number, and to be doublet if it is odd. Again we have one exception, $^3O_2$, which is just mentioned above.

Table S2: System components used to estimate the energy profile.

	Core	Coefficients of the second group components									
		H_2O	EBf–e$^-$	EBf	PBf–H$^+$	PBf	XEA–e$^-$	XEA	XPA–H$^+$	XPA	O_2
K_0	^{3}[D11]	2	1	0	1	0	0	4	0	4	0
K_{02}	^{2}[D12]$^+$	2	1	0	1	0	1	3	0	4	0
K_{03}	^{2}[D13]$^+$	2	1	0	1	0	1	3	0	4	0
K_{04}	^{2}[D14]	2	1	0	1	0	1	3	1	3	0
K_1	^{3}[D11]	2	0	1	0	1	1	3	1	3	0
K_{12}	^{2}[D12]$^+$	2	0	1	0	1	2	2	1	3	0
K_{13}	^{2}[D13]$^+$	2	0	1	0	1	2	2	1	3	0
K_{14}	^{2}[D14]	2	0	1	0	1	2	2	2	2	0
K_{15}	^{3}[D15]	2	1	0	1	0	2	2	2	2	0
K_2	^{3}[D21]	1	1	0	1	0	2	2	2	2	0
K_{22}	^{2}[D22]$^+$	1	1	0	1	0	3	1	2	2	0
K_{23}	^{2}[D23]$^+$	1	1	0	1	0	3	1	2	2	0
K_{24}	^{2}[D24]	1	1	0	1	0	3	1	3	1	0
K_3	^{3}[D21]	1	0	1	0	1	3	1	3	1	0
K_{32}	^{2}[D22]$^+$	1	0	1	0	1	4	0	3	1	0
K_{33}	^{2}[D23]$^+$	1	0	1	0	1	4	0	3	1	0
K_{34}	^{2}[D24]	1	0	1	0	1	4	0	4	0	0
K_{35}	^{3}[D25]	1	1	0	1	0	4	0	4	0	0
K'_0	^{1}[D11]	0	1	0	1	0	4	0	4	0	1

S2.2 System components to estimate the energy of intermediates

The total energies of the K-states and intermediates are estimated by summing up the energies of the first group and the second group as shown in Table S2. The total number of electrons and nuclei are conserved throughout. Note that K_{n1} ($n = 0, 1, 2, 3$) is missing in Table S2. It has the same components K_n but in the electronic excited states, which is corresponding to the result of the CPEWT. The energy is estimated from the result of nonadiabatic electron-wavepacket dynamics shown in the main text.

References

[1] K. Takatsuka, T. Yonehara, K. Hanasaki, and Y. Arasaki, *Chemical Theory Beyond the Born-Oppenheimer Paradigm: Nonadiabatic Electronic and Nuclear Dynamics in Chemical Reactions*, World Scientific, Singapore, 2015.

[2] K. Yamamoto and K. Takatsuka, *ChemPhysChem*, 2015, **16**, 2534–2537.

[3] K. Yamamoto and K. Takatsuka, *Chem. Phys.*, 2016, **475**, 39–53.

[4] K. Yamamoto and K. Takatsuka, *ChemPhysChem*, 2017, **18**, 537–548.

[5] P.-O. Löwdin, *J. Chem. Phys.*, 1950, **18**, 365–375.

[6] R. S. Mulliken, *J. Chem. Phys.*, 1955, **23**, 1833–1840.